**Journal of Mining and Earth Sciences**

Journal homepage: http://tapchi.humg.edu.vn/en/home.html

# Numerical simulation of wave propagation in rock media: The effect of element type on the boundary condition and the analysis result in a model of blast vibration

**Dang Van Kien**
*Hanoi University of Mining and Geology, Vietnam*
*Tel.:* +84 983080325; *Email:* kienxdn@gmail.com

ARTICLE INFO

*Article history:*
Received 11 September 2015
Accepted 21 November 2016
Available online 30 July 2016

*Keywords:*
Numerical analysis
Boundary condition
Infinite element
Blast vibration
Existing tunnel

ABSTRACT

In finite element method (FEM), the selection of boundary condition types will affect on the results of a model. The boundary condition depends on the type of boundary elements. In the wave propagation in rock/soil medium such as blast vibration in tunnel blast, fixed or roller or non-reflecting boundary conditions can be used. The boundary element, used fixed or roller boundary conditions, is finite elements. The wave may be reflex when propagating to boundary. Non-Reflecting Boundary Conditions (NRBCs) are used to model a problem with an infinite domain by using a finite model. Many types of NRBCs are available, but, in general, they all act to prevent energy radiating toward infinity from being reflected back into the model at the finite boundary of the model. Infinite elements are another method of imposing a NRBC in a finite element method model. The concept of infinite elements is to use finite elements to define a semi-infinite domain at the boundary which is desired to be a NRBC. In this paper, the finite element method is used to study the blast wave propagation by using two types of boundary conditions: fixed condition and non-reflecting boundary condition. In the first model, there are only finite elements (FE). On the contrary, both finite and infinite elements (FE+IE) are used in the second model. The comparison of the results of these models is presented to show the effect of used element type.

## 1. Introduction

The wave propagation phenomenon is an important subject in the field of geotechnical engineering where soil/rock media have to be treated as continua. Dynamic disturbances are described well in the viewpoint of wave propagation. Numerical simulation studies of wave propagation show that one of the most difficult parts of the problem is the simulation of boundaries. This is the main point that makes soil/rock dynamics more difficult than structural dynamics since the waves at the boundary must radiate and not return to the medium of interest. Efficient modeling of infinite media is important for many engineering problems. In this work the coupled computational methods of finite and infinite elements are used to simulate the wave propagation problem.

## 2. In situ monitoring result

The blast vibration during tunnel excavation at Croix-Rousse tunnel (Lyon, France) was measured by sensors (Geophone type). The sensors are located in concrete tunnel lining along the tunnel and some places

on some buildings on the surface. The results of blast particle velocity are presented in three directions: transverse direction, vertical direction and along the tunnel (Dang et al., 2013), as shown in Figure 1. By located sensors in buildings, the results of peak particle velocity are presented in Table 1. These results indicate the peak particle velocity is smaller than the velocity threshold of France (after AFTES). The results will be verified by numerical simulation model.

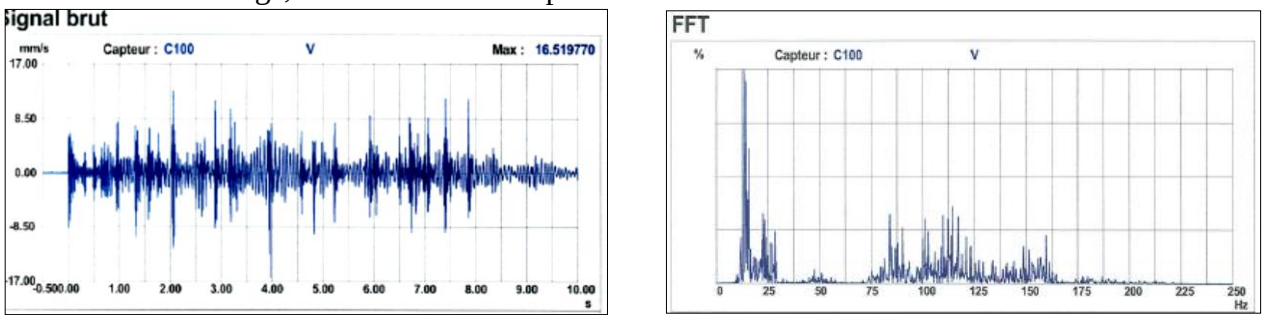


*a. The velocity and frequency spectrum in x axis*

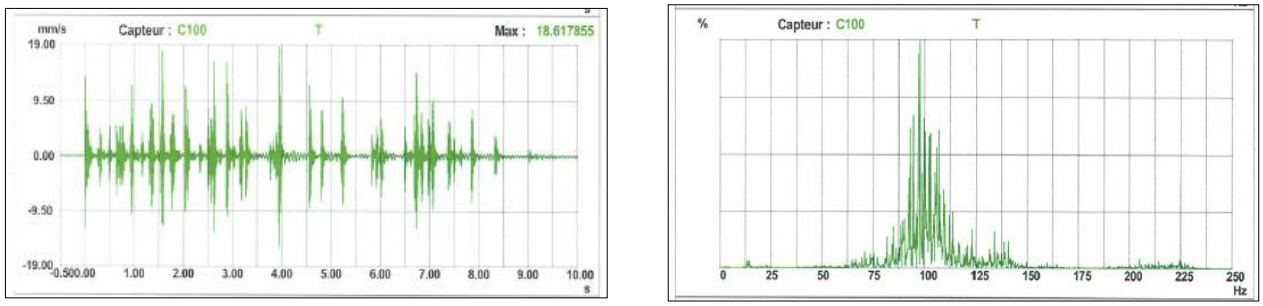


*b. The velocity and frequency spectrum in y axis*

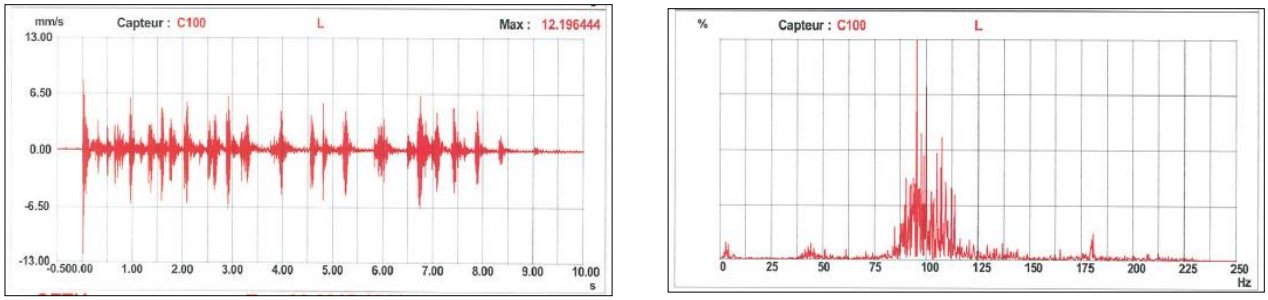


*c. The velocity and frequency spectrum in z axis*

*Figure 1. The measuring of velocity and frequency spectrum of the above blast signal*

*Table 1. The result of some sensors at some buildings on the surface*

| Name/ location of sensor | PM | Cover (m) | PPV (mm/s) |
|---|---|---|---|
| S12 /Ventilation factory n°1 | 225 | 60 | 1,77 |
| S20/ Ventilation factory n°2 | 555 | 65 | 0,66 |
| S21/ Rousy street | 585 | 68 | 3,76 |
| S22/77 Bd Cx Rousse | 680 | 72 | 7,97 |
| S25/99 Bd Cx Rousse | 870 | 78 | 2,71 |
| S26/94 Bd Cx Rousse | 685 | 72 | 2,25 |

## 3. Numerical simulation

### *3.1. Method*

Numerical simulation model is carried out by using the FEM through the use of Abaqus/explicit 6.11-2.

*3.1.1. The Dynamic Equilibrium Equation*

Dynamic simulation with any numerical method essentially involves the solution of the equations of motion. In a finite element formulation, these equations can be written in (Hughes, T. J. R., 2000) as

$$[M]\{\ddot{u}\}+[C]\{\dot{u}\}+[K]\{u\}=\{P(t)\}, \quad (1)$$

where $u$ - displacement, $\dot{u}$ - velocity, and $\ddot{u}$ - acceleration.

The mass matrix:

$$[M]=\int_v \rho[N]^T[N]dV, \quad (2)$$

In the above equations, ρ is the material density and [N] is the shape function matrix. The damping matrix, [C], for the Rayleigh damping is in the form:

$$[C]=\alpha[M]+\beta[K], \quad (3)$$

where α and β are pre-defined constants. The time-dependent stiffness matrix is defined as

$$[M]=\int_v B^T[D][B]dV, \quad (4)$$

[D] and [B] represent the constitutive and strain-displacement matrices, respectively. The nodal force vector due to surface tractions, [q(t)], and body forces, [f(t)], is given by

$$\{P(t)\}=\int_S [N]^T q(t)S+\int_V [N]^T f(t)V, \quad (5)$$

The Equation (1) can be re-written in the following form:

$$[M]\{\ddot{u}\}=\{f^{ext}\}-\{f^{\text{int}}\}, \quad (6)$$

where,

$\{f^{ext}\}=P(t)$ and $\{f^{\text{int}}\}=[C]\{\dot{u}\}+[K]\{u\}$

Equations (1) and (6) can be solved either by explicit methods in which the most popular one is the central difference method or by implicit methods such as Hubolt algorithm, Nemark algorithm. Solutions by explicit methods require finding an initial solution for a set of algebraic equations. No global matrix formulation is needed in the explicit methods and no iterations are performed.

The most efficient explicit dynamic analysis procedure is the second order central difference operator, which is based on the implementation of an explicit integration rule together with the use of diagonal or lumped element mass matrix. Half-time step values are used to calculate velocity and acceleration. Both values are accurate to an order of $t^2$ (time step square). Values of the derivatives at the center of a time interval are obtained from the difference in the function values at the ends of the interval. The central difference integration operator is explicit in which the kinematic state may be advanced by using known values of $\dot{u}^{(i-\frac{1}{2})}$ and $\ddot{u}^{(i)}$ from the previous time increment. A key to the computational efficiency of the explicit solution procedure is the use of diagonal element mass matrices. Because the inversion of matrices required in the beginning of each time increment, makes the solution of algebraic equations very simple. Thus, the Equation (6) can be written as

$$[M]\{\ddot{u}\}=[M]^{-1}(\{f^{ext}\}-\{f^{\text{int}}\}) \quad (7)$$

The explicit procedure integrates through time by using many small increments. The central difference operator is conditionally stable and stability limit for the operator (with no damping) is given in terms of the highest eight values in the system as (ABAQUS, 2011).

$$\Delta t \le \frac{2}{\omega_{\max}}, \quad (8)$$

where $\omega_{\max}$ is the circular frequency of the natural modes. With damping, the stable time increment is given by (ABAQUS, 2011).

$$\Delta t \le \frac{2}{\omega_{\max}}(\sqrt{1+\xi_{\max}^2}-\xi_{\max}), \quad (9)$$

where $\xi_{\max}$ is the fraction of critical damping in the mode with the highest frequency (test dimension of element or test the stability of method). The current dilatational wave speed in the element is calculated with the following expression:

$$C_d=\sqrt{\frac{(\hat{\lambda}+2\hat{\mu})}{\rho}}, \quad (10)$$

where $\hat{\lambda}$ and $\hat{\mu}$ are effective Lamé constants and material's mass density, respectively.

*3.1.2. Description of Numerical Model*

The numerical model was carried for investigating the blast vibration of a newly excavated tunnel which is constructed by blasting method at nearby existing tunnel. The model includes three parts: the rock mass is 160m in length and 160m in width, the boundary of model is created by infinite element with 160m in length. The existing tunnel is a vaulted roof with a vertical wall. The radius of the arch is 8,05m and vertical wall is 1,0m. The newly excavated tunnel is round with the radius of the arch of 5,55m. Distance between two tunnels is 42,6m. The dimension of the model is 480m in width and 320m in height. The dimension of the 2D model of case study is presented in Figure 2 and Figure 3.

***3.2. Boundary Condition***

In this paper, we investigate on two cases with different boundary elements and boundary conditions.

Case 1: Non-reflecting boundary condition with Finite/Infinite Elements in Figure 2.

Case 2: Fixed boundary condition with only Finite Elements in Figure 3.

Infinite elements are used to create non-boundary conditions for models. With these boundaries, there is no reflecting of wave at boundaries. In 2D model, coupled finite-infinite elements are used including of the types of CPE4R and CINPE elements. The top surface is free and other three surfaces are non-reflecting boundaries which are created by the type of the CINPE infinite element.

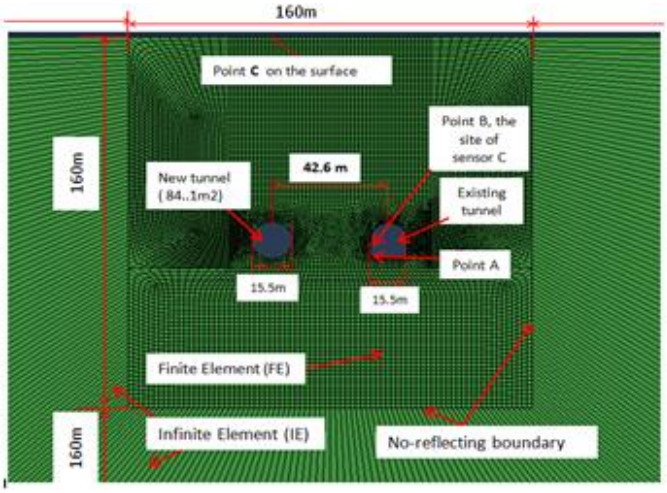


*Figure 2. The dimension of 2D model of case 1*

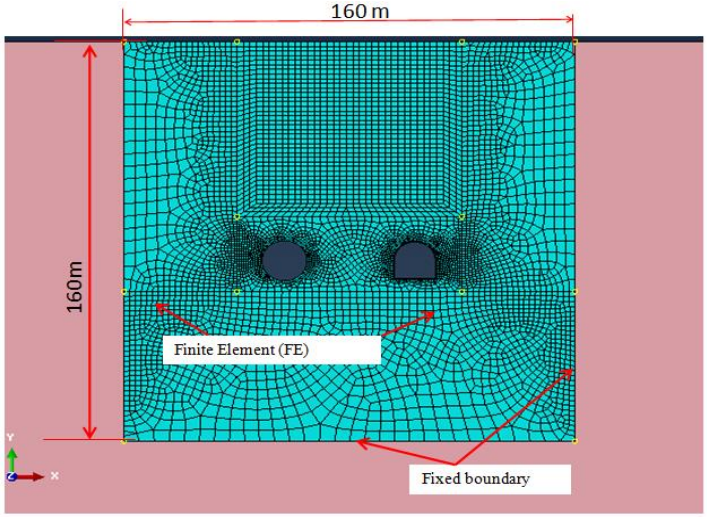


*Figure 3.The dimension of 2D model of case 2*

### *3.3. Validation of the mesh: Rayleigh velocity*

The velocity of Rayleigh wave is used to validate the mesh in numerical simulation [Edip et al., 2011]. The dimension of the model is 480m in width and 320m in height in Figure 4. The finite element is CPE4R, a 4-node bilinear plane strain quadrilateral, reduced integration, hourglass control. The infinite element is CINPE4 (IE), 4-node linear and one-way infinite. The length of this element is chosen as 160m. With the average size of an element of 0,5m, the total number of elements is 103360 (102400 linear quadrilateral elements of type CPE4R and 960 linear quadrilateral elements of type CINPE4). A force depending on time is applied to a point in which the distance from the located point of the force to the boundary is 5m. The magnitude of load is 1500GPa and the relation between load and time is presented in Figure 5.

In order to simulate surface wave propagation in 2D, the velocity of Rayleigh wave propagation is considered. The result of the Rayleigh wave velocity at point B and point C is presented in Figure 6.

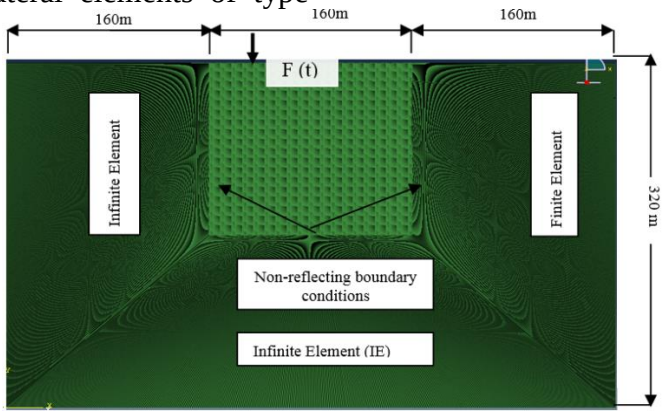


*Figure 4. Domain discretization-finite & infinite element*

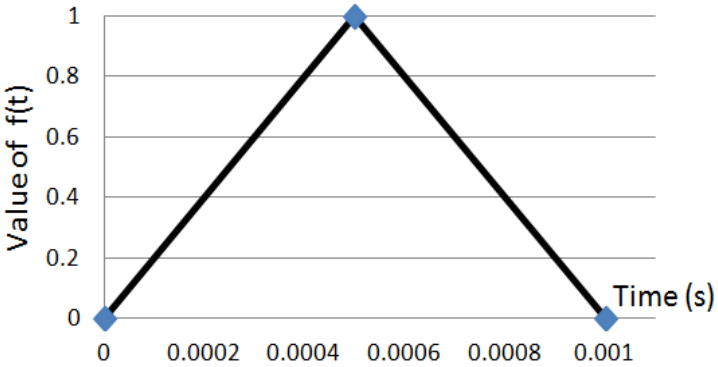


*Figure 5. The force load versus time*

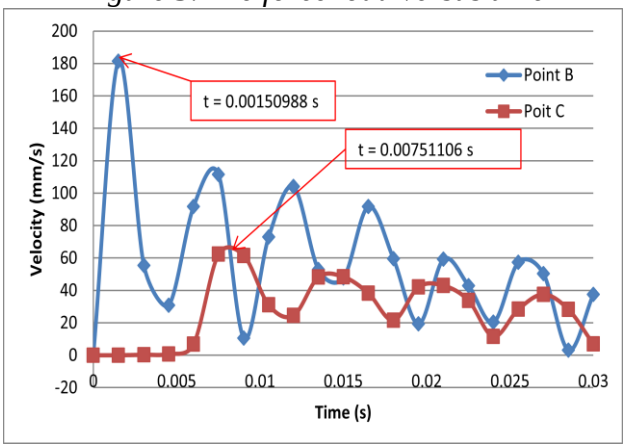


*Figure 6. The time velocity history*

The material dynamic parameters of rock mass are selected: Young's modulus is 56GPa, Poisson's ratio is 0,33, and density is 2650 kg/m$^3$. As shown in Figure 6, the time difference between point B and point C is 0,00600117s as the distance between them is 18,5m. Then, the velocity of Rayleigh wave is calculated S/t=3082,72968m/s. The velocity of Rayleigh wave can be calculated by the formula of Bergmann-Viktorov, or

$$V_R = \left( \frac{0,87 + 1,12\nu}{1+\nu} \right).V_S(m/s) \quad (11)$$

where ν is the Poisson's ratio, $V_S$ is the S-wave velocity which is given by the formula (Nesvijski, E. G., 2009) as

$$V_S = \sqrt{\frac{G}{\rho}} = \sqrt{\frac{E}{2(1+\nu)}}(m/s) \quad (12)$$

From the formula in Equations (11) and (12), the values of $V_S$ and $V_R$ can be calculated as $V_S$ = 3218 m/s and $V_R$ = 2999 m/s. The difference of velocity values between two methods (theory method and numerical simulation) is not large and about 2,71 %. The mesh is convergent. This mesh is used for modeling the effect of blast vibration by tunnel excavation on existing tunnel and building on the surface.

### *3.4. Blast loading model*

The explosion pressure, which is the pressure exerted by the expansion of gases from the explosion, can be calculated from the following equation, as suggested by the Konya and Walter (1991) as

$$P_d = \frac{449,93 x SG_e x VOD^2}{1 + 0,8 SG_e}, \quad (13)$$

where $P_d$ is the detonation pressure (Pa), $SG_e$ the density of the explosive (g/cm$^3$), and VOD is the detonation velocity of the explosive (m/s).

The detonation pressure is the pressure of a fully coupled charge completely filling the blasthole. In the field, the decoupling technique is used which refers to leaving an empty space between an explosive column and the blasthole wall. For consideration of the decoupling effect, the following calibration equation was used (DANG Van Kien et al., 2012).

$$P_B = P_d \left( \frac{d_c}{d_h} \right)^3, \quad (14)$$

where $P_B$ is the blasthole pressure considering decoupling ($P_B$), $d_c$ and $d_h$ are the diameters of the explosive and blasthole (mm), respectively. To obtain the pressure-time profile of the explosion gases, the wave-shape function is needed. Most researchers have used exponential functions to model the wave-shape of explosive pressure and introduced a combination of exponential and sinusoidal functions as the pressure function. In the present study, the following wave-shape function, based on the equation by Jiang (1993), was adopted to characterize the source of vibration (Park et al 2004).

$$f(t) = \frac{t}{t_d} e^{\left(1 - \frac{t}{t_d}\right)}, \quad (15)$$

where f(t) is the shape function, t is the elapsed time, and $t_d$ = 0,0003361s is the time to reach the peak pressure. The relation between f(t) and t can be seen in Figure 7.

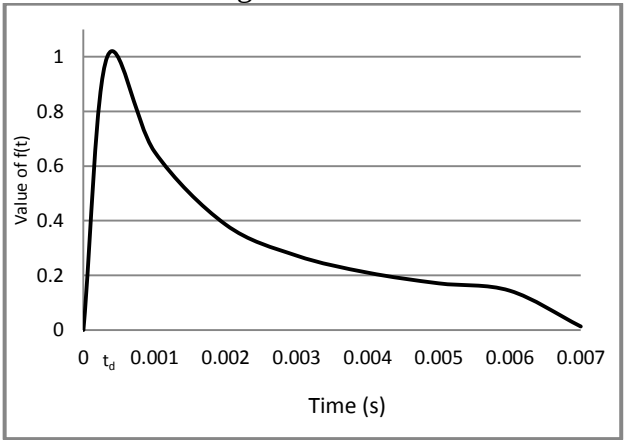


*Figure 7. Blast load versus time (Park et al., 2004)*

A radial force, equivalent to the blasthole pressure, is applied to the particles around the blasthole. To prevent the generation of an irregular force around the blast hole due to the coarse particle size, the particles around the blasthole had a radius smaller than that of the surrounding particles. Figure 7 shows the propagation of applied blast pressure. The Emulsion Reelle explosive was used to excavate the tunnel with ($d_c/d_h$ = 0,9). The amplitude pressure is calculated from the

formula (14) and the perimeter of the tunnel is given by

$P_B = 7{,}478Gpa$

$$P(t) = P_B * f(t) = 7{,}478 * f(t); \quad (16)$$

### *3.5. Material model*

The rock mass surrounding the Croix-Rousse tunnel is granite and gneiss rock. The traditional Mohr-Coulomb critical is used to study the rock damage process. The dynamic parameter properties of rock are Bulk modulus = 56GPa, cohesion = 23,07MPa, density = 2650 kg/m$^3$, friction angle 53,99$^0$, dilation angle = 4$^0$. The damping ratios are chosen to be α = 0,01 and β = 0,02 for both rock and concrete. The concrete lining was simulated by using the concrete damaged plasticity model built into Abaqus. The material properties used for concrete: Young's modulus is 31GPa, Poisson's ratio is 0,2, density is 2400kg/m$^3$, the compressive yield strength is 35MPa and tensile yield is 2,9MPa.

## 4. Result analysis

The stresses in rock mass in case 1 at t = 0,01s and t = 0,015s are presented in Figure 8. At t = 0,015s, one can see the reflecting stress wave in the rock mass. The stress wave in rock mass of case 1 is presented in Figure 8. The velocity and displacement at point A, point B, and point C are presented in Figure 9. In case 2, there is not reflecting wave stress in rock mass, as shown in Figure 10, the velocity and displacement at point A, point B, and point C are presented in Figure 12. Comparison the velocity and displacement value between two cases are made. The results for comparison are presented in Figure 13. We can see the velocity values in case 2 are the same as these values in situ recording result. The velocity and displacement values in case 2 are smaller than these values in case 1.

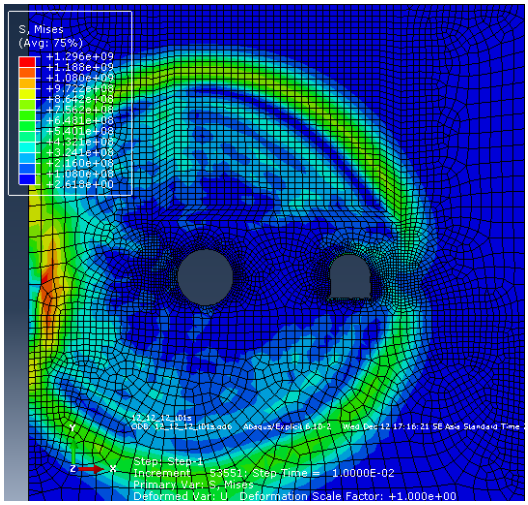


*a. The stress wave in rock mass in case 1 at t= 0,01s*

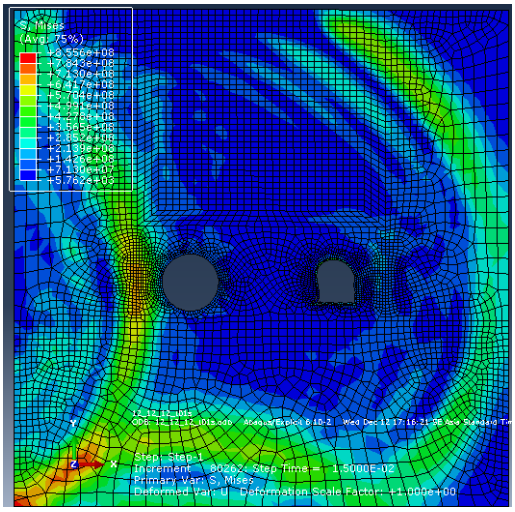


*b. The stress wave in rock mass in case 1 at t= 0,015s*

*Figure 8. Case 1-Using the Fixed boundary condition (FE only)*

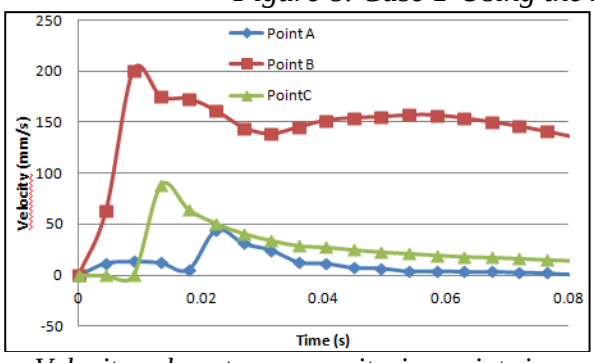


*a. Velocity value at some monitoring points in case 1*

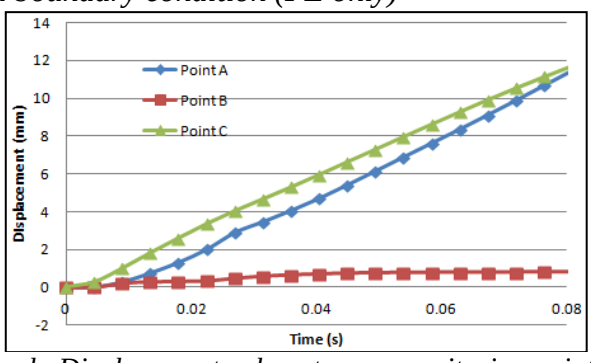


*b. Displacement value at some monitoring points in case 1*

*Figure 9. Result of velocity and displacement value in case 1(FE only)*

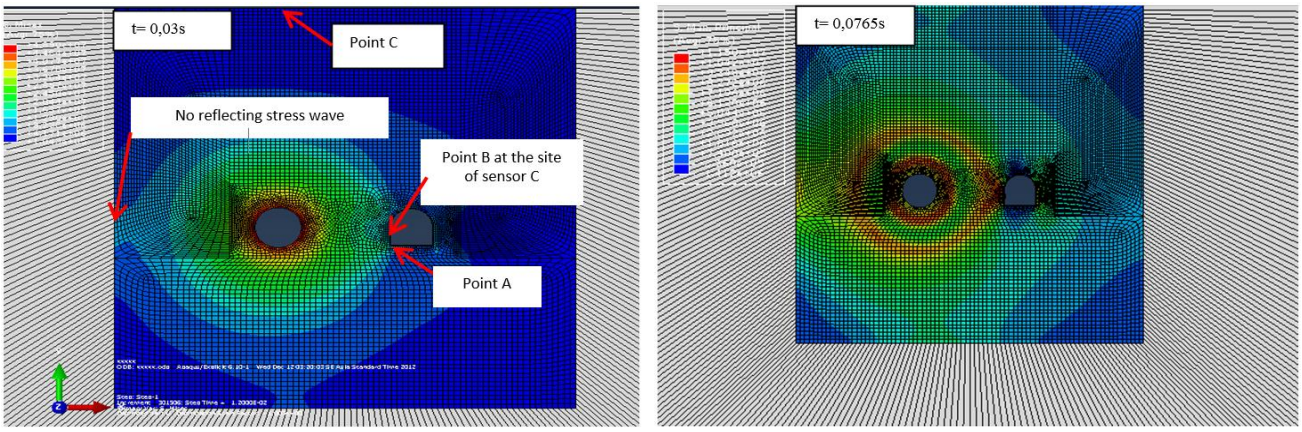


*a. Stress wave in rock mass in case 2 at t= 0,03s* *b. Stress wave in rock mass in case 2 at t= 0,0765s*

*Figure 10. Case 2-Using the NRBCs by Finite/Infinite Element (FE+IE)*

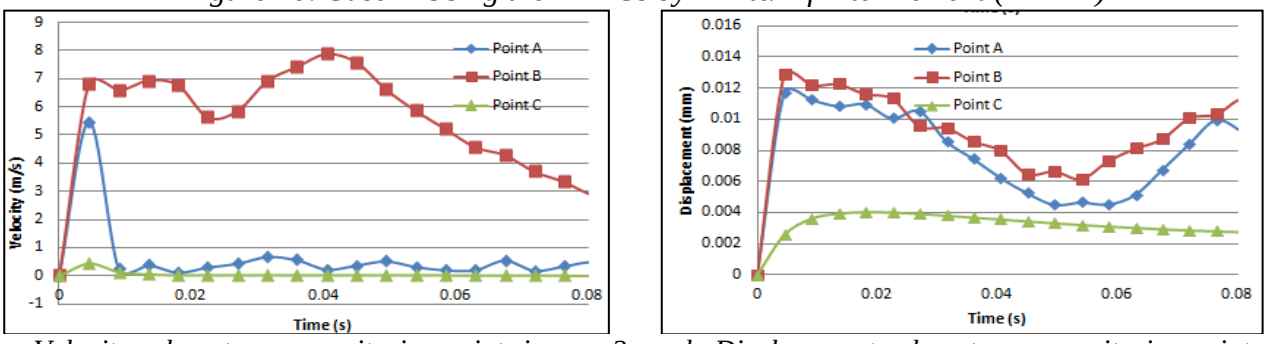


*a. Velocity value at some monitoring points in case 2* *b. Displacement value at some monitoring points in case 2*

*Figure 11. Result of velocity and displacement value in case 2*

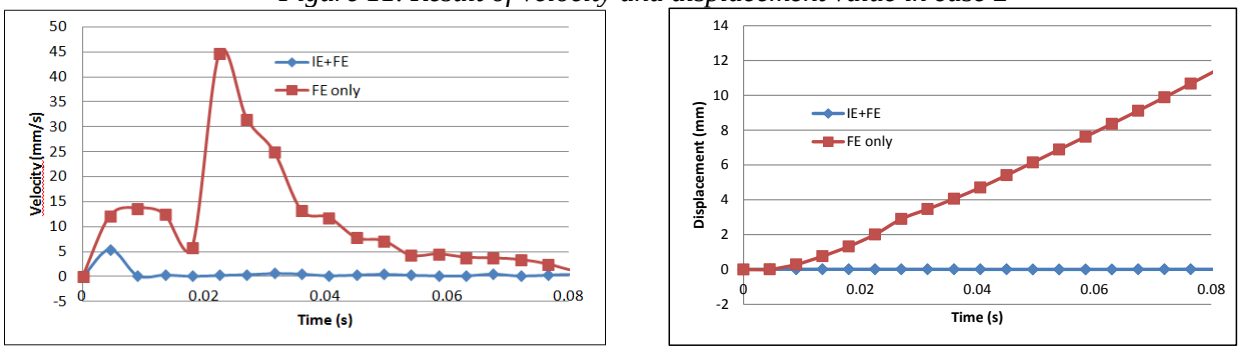


*a. Compare the velocity values between two cases* *b. Compare the displacement values between two cases*

*Figure 12. The comparison of the velocity and displacement values between two cases*

## 5. Conclusion

From the analysis and simulation results in the paper, the following conclusions are drawn:

- The velocity and displacement values in case 2 (Non-reflecting boundary using IE+EF) are smaller than these values in case 1 (Fixed boundary condition using FE only).
- The difference of results depends on the boundary condition type, the time period, the point of monitoring, and the area of limited region for calculating.
- The reason of the difference is the reflecting stress wave in case 1.
- The usage of infinite elements can improve the results significantly.

**Acknowledgment**

The author would like to thank Prof. Trong Hung Vo and Dr. Ngoc Anh Do for the help given during the preparation of the work. The author would like to thank the reviewer for their valuable comments and suggestions to improve the quality of the paper.

## REFERENCES


ABAQUS User's Examples and Theory Manual, version 6.10, Simulia, Providence, 2011.

Chen, S. G. et al, 2000. Discrete element modelling of an underground explosion in a jointed rock mass. Geotechnical and Geological Engineering, 18: 59-78.

Clayton, E., Soler, B., Voiron, J., 2011. Renovation of Croix. Rousse tunnel - Specific points of the technical design, AFTES. Congrès International, Lyon1, page 135.

Da-neng, L., 2011. The mitigation negative effect of tunnel-blasting-induced vibrations on existing tunnel and buildings. Journal of coal science & engineering, 2011, Vol.17 No.1 Mar.2011. DOI 10.1007/s12404-011-0106-4.

Dang, V.K. Limam, A., Surin, D., Humbert, E., 2013. Blast vibration induced during tunnel excavation in urban areas: Numerical simulation and measure results. Conference Franco –Vietnamienne CIGOS 2013 Construction et Developpement Durable. 04-05, Avril 2013, Lyon, France.

Dang Van Kien, 2008. The construction situation of shaft in mining and construction industry in Vietnam, Proceeding of the international conference on advances in mining and tunneling, Organizers by Hanoi University of Mining and Geology and TU Bergakademie Freiberg, Germany. 20-21 August 2008, Hanoi, Vietnam, pp.227-237.

DANG Van Kien, HUANG Ge-Jia, VU Xuan Hong, Frederic PELLET, 2012, Experimental and numerical investigations of the Split Hopkinson test on granite rock. Proceeding of the international conference on advances in mining and tunneling. Organizers by Hanoi University of Mining and Geology and TU Bergakademie Freiberg, Germany. 20-21 August 2012, Hanoi, Vietnam, pp.263-271.

Hughes, T. J. R., 2000. The finite element method: linear static and dynamic finite element analysis. Dover publications, NY, page 682.

Dohyun Park, Byungkyu Jeon, Seokwon Jeon, 2009. A Numerical Study on the Screening of Blast-Induced Waves for Reducing Ground Vibration. Rock Mech Rock Eng (2009) 42:449–473. DOI 10.1007/s00603-008-0016-y.

Edip, K. et al., 2011. Numerical simulation of wave propagation in soil media. Proceedings of the 21st European Young Geotechnical Engineers' conference. Rotterdam, 140-145.

Ngo Doan Hao, Dang Van Kien, Nguyen Van Tri, 2008, Smooth blasting design for drifts excavation by using KNMTB1.0 software, Proceeding of the international conference on advances in mining and tunneling, Organizers by Hanoi University of Mining and Geology and TU Bergakademie Freiberg, Germany. 20-21 August 2008, Hanoi, Vietnam, pp.187-192.

Nesvijski, E. G., 2009. On a Possibility of Rayleigh Transformed Sub-Surface Waves Propagation. The e-Journal of Nondestructive Testing & Ultrasonics. Issue Vol. 5 No. 9.

M. Keshavarz, V.K. Dang, K. Amini Hosseini, F.L. Pellet 2013, AE thresholds and compressive strength of different crystalline rocks subjected to static and dynamic loadings, 1st International Conference on Rock Dynamics and Applications. 06-08 June 2013, Lausanne- Switzerland, pp.213-218.

Park BK, Lee IM, Kim SG, Lee SD, Cho KH., 2004. Probabilistic estimation of fully coupled blasting pressure transmitted to rock mass. II: Estimation of rise time. Tunnelling Technol 6(1):25–39.

F. L. Pellet, V. K. Dang, C. Baumont, M. Dusseux, G. J. Huang, 2013. Determination of dynamic rock strength to assess blasting efficiency, International conference on Rock Mechanics for Resources, Energy, and Environment- Eurock 2013. 21-26 September 2013, Wroclaw, Poland, ISBN: 978-1-138-00080-3, DOI: 10.1201/b15683-129,pp.757-7.